SCIENCE CHINA
Information Sciences

• RESEARCH PAPER •

December 2024, Vol. 67, Iss. 12, 222203:1–222203:17
https://doi.org/10.1007/s11432-023-4153-8

Time-varying formation tracking control of high-order multi-agent systems with multiple leaders and multiplicative noise

Ruru JIA[1,2], Xiaofeng ZONG[2,3*] & Qing WANG[4]

[1]*College of Artificial Intelligence, Nankai University, Tianjin* 300350, *China;*
[2]*School of Automation, China University of Geosciences, Wuhan* 430074, *China;*
[3]*Hubei Key Laboratory of Advanced Control and Intelligent Automation for Complex Systems, Wuhan* 430074, *China;*
[4]*School of Automation Science and Electrical Engineering, Beihang University, Beijing* 100191, *China*

Received 19 December 2023/Revised 15 February 2024/Accepted 22 May 2024/Published online 12 December 2024

Abstract This work discusses the time-varying formation (TVF) tracking control problem of high-order multi-agent systems (MASs) with multiple leaders and multiplicative measurement noise. With the help of Lyapunov function tools and stochastic analysis methods, the TVF tracking protocol with multiple leaders and multiplicative noise is developed based on the relative state measurements, where followers are driven to realize the target TVF while tracking the convex combination formed by multiple leaders. Then, the TVF tracking problem is converted into the mean square asymptotic stability problem of a stochastic differential equation (SDE); sufficient conditions related to the control gains are given by stabilizing the corresponding stochastic system. Moreover, a TVF tracking algorithm is presented to outline the steps of protocol design. Finally, the theoretical results are illustrated in terms of simulation examples.

Keywords multi-agent systems, multiple leaders, multiplicative measurement noise, stochastic differential equation, formation tracking control

1 Introduction

Recently, formation control problems of multi-agent systems (MASs) have aroused enormous interest owing to both their research challenges and practical potential in various fields, such as autonomous underwater vehicles (AUVs) [1,2], mobile robots [3–5], unmanned aerial vehicles (UAVs) [6,7], spacecraft and satellites [8], etc. At present, there exist several classical methods that can drive the MASs to realize the target formation, such as the virtual structure method [9], leader-follower method [10–13], behavior-based method [5], and consensus-based method [14, 15]. For a large-scale MAS, centralized formation strategies are not suitable owing to the limitation of calculation and communication performance. Hence, one has to resort to distributed formation strategies such as the consensus-based formation strategy.

Consensus-based formations mean that all agents update their states by using neighboring relative information and eventually tend to the specified formation. Ren [16] presented a second-order consensus strategy for solving vehicle formation control problems and demonstrated the superiority of this strategy. Cao and Ren [17] provided a consensus formation algorithm of fractional-order systems and gave convergence conditions. In [18], the control protocol design and time-varying formation (TVF) analysis for high-order MASs with communication delays were proposed. The aforementioned formation control problems focus on the specified situation in which MASs accomplish the single formation task together. However, in many practical situations, MASs are requested to build several groups, such as target enclosing, to perform more complex tasks.

In the multiple leaders' case, Dong et al. [19, 20] investigated formation-containment control issues and proved that containment issues, consensus issues, consensus tracking issues, and formation tracking issues can all be viewed as special situations of formation-containment issues. For high-order swarm

* Corresponding author (email: zongxf@cug.edu.cn)

systems subject to unknown disturbances and switching topologies, a distributed group TVF tracking strategy was proposed by the adaptive control method in [21], where agents were classified as the follower, the group leader, and the virtual leader. Su et al. [22] developed a stochastic sampling mechanism for realizing TVF tracking controls of linear MASs with time delays and derived sufficient conditions. Based on consensus theory, the TVF tracking methods of high-order and second-order MASs under the directed interaction graph were presented in [23] and [24], respectively. Against state-dependent uncertainties and actuator faults for nonlinear MASs under multiple leaders, a fault-tolerant TVF tracking strategy was constructed in [25] and the stability was verified by the Lyapunov-like function.

Note that the above works are based on the ideal communication assumption. In realistic scenarios, MASs often work in uncertain communication environments and are easily disrupted by stochastic noises, which can influence system performance and even cause instability. For example, multiplicative noises often occur in the modeling of communication process, especially for the cases of fading communication channels [26, 27]. In this situation, multiplicative noises and additive noises were studied in [26–29] when solving consensus problems of MASs. In [30–32], additive noises were considered in the distributed formation controls. For high-order MASs subject to additive measurement noises and markovian switching topologies, a stochastic approximation protocol was proposed to accomplish TVF in [33]. Shames et al. [34] developed an anchors select mechanism to minimize the influence of additive noise on the localization of MAS autonomous formation. For high-order MASs with multiplicative noises, a TVF strategy was proposed in [35], where sufficient conditions were deduced by the Lyapunov function and the Lyapunov functional method . Significantly, the formation controls for MASs with noises in [30–35] only consider the situation without a leader, which makes it difficult for existing algorithms to settle complex practical matters such as target tracking. Hence, the TVF tracking problem of high-order MASs with multiple leaders in noisy environments should be addressed.

Inspired by the previous works [23, 24], where the TVF tracking problem was investigated for the deterministic systems, this work discusses the TVF tracking problem for high-order MASs with multiple leaders and stochastic measurement noise in the directed topology. Different from the deterministic systems in [21–25], the closed-loop MAS with multiple leaders and multiplicative measurement noise is actually a SDE, whose stability analysis is more difficult and complex. Hence, we can not apply the skills in deterministic systems to current work directly. In our work, the stochastic stability of SDEs is established to realize the TVF tracking and design the control protocol under multiple leaders and multiplicative measurement noise. The main contributions are listed in three aspects.

(1) A novel TVF tracking protocol and its overall control structure are presented for high-order MASs with multiplicative measurement noise and multiple leaders in uncertain communication environments. Compared with existing TVF tracking results in deterministic systems [21–25], this article takes the stochastic multiplicative noise into account to make this protocol more general and significant in realistic scenarios. The simulation results demonstrate that compared to [23], our results have better robustness even in the presence of noise interference, which is reflected in smaller overshoots and fewer oscillations before achieving the TVF tracking.

(2) Different from the formation control and consensus control problems without a specific leader or with only one leader under noisy environments in [26–35], the TVF strategy with multiple leaders is provided in stochastic settings. Due to the latent conflict between protecting the target TVF and tracking multiple leaders, this issue shows more interest and challenge than those formation works in [30–35].

(3) Two new techniques (Theorems 2 and 3) are developed to investigate the mean square TVF tracking for MASs under multiplicative noise and multiple leaders. Because the presence of stochastic noise allows our problem to be discussed in the background of probability, the methods of deterministic TVF tracking controls [21–25] are not applicable and cannot be directly extended to this article. We establish the stochastic stability of corresponding SDEs and apply it to our TVF tracking problem. This "robust" result is a new supplement to the stability theory of stochastic differential systems. Moreover, we also present a TVF tracking algorithm to outline the steps of protocol design.

The rest of this work makes arrangements as follows. Section 2 presents some math preliminaries. For MASs with multiple leaders and multiplicative noise, Section 3 presents sufficient conditions to realize the mean square TVF tracking. Section 4 gives simulation examples for the proposed method. Section 5 summarizes this paper.

Notation: $\otimes$ represents the Kronecker product. 0 represents the zero matrix. Denote by I_N the N-dimensional identity matrix. For any given vector or matrix A, $\|A\|$ represents the Euclidean norm, A^T represents its transpose, $\max(\mathrm{Re}(\lambda(A)))$ represents the maximum real part of eigenvalues. For any

matrix B, $\lambda_{\max}(B)$ represents the maximum eigenvalue and $\lambda_{\min}(B)$ represents the minimum eigenvalue. diag$\{\cdot\}$ denotes a diagonal matrix. For continuous martingales $G(t)$ and $H(t)$, $\langle G, H\rangle(t)$ denotes their joint quadratic variation. For any vector or variable X, the mathematical expectation is represented as $\mathbb{E}X$. $(\mathbf{\Omega}, \mathbf{F}, \mathbf{P})$ represents the complete probability space. For symmetric matrices A and B, $A > B$ (respectively, $A \geqslant B$) signifies that the matrix $A - B$ is positive definite (respectively, positive semidefinite).

2 Preliminaries

We first introduce preliminaries of the graph theory and present the problem description. When the TVF tracking control for MASs under multiple leaders and multiplicative measurement noise is studied, the formation tracking problem of MASs is converted into a stochastic stability problem of SDEs. Therefore, we establish the stochastic stability theorem (see Theorem 1).

2.1 Graph theory

We consider a MAS with N agents. The directed graph is expressed by $\mathcal{G} = \{\mathcal{V}_\mathcal{G}, \mathcal{E}_\mathcal{G}, \mathcal{A}_\mathcal{G}\}$, where $\mathcal{V}_\mathcal{G} = \{v_1, v_2, ..., v_N\}$ is the node set with v_i being the ith agent, $\mathcal{E}_\mathcal{G}$ represents the set of edges, and $\mathcal{A}_\mathcal{G} = [a_{ij}] \in R^{N\times N}$ denotes the adjacency matrix with nonnegative elements. The $e_{ij} = (v_i, v_j)$ denotes the edge of $\mathcal{G}$. For $\mathcal{A}_\mathcal{G}$, if e_{ij} belongs to $\mathcal{E}_\mathcal{G}$, the adjacency element $a_{ij} = 1$, otherwise $a_{ij} = 0$. Let $\mathcal{N}_i = \{v_j \in \mathcal{V}_\mathcal{G} : (v_j, v_i) \in \mathcal{E}_\mathcal{G}\}$ be the neighbour set of v_i, which indicates that v_i can receive information from v_j. In addition, the in-degree of node v_i is represented by $\deg_{in}(v_i) = \sum_{j=1}^{N} a_{ij}$. The Laplacian matrix of directed graph $\mathcal{G}$ is denoted by $\mathcal{L}_\mathcal{G} = \mathcal{D}_\mathcal{G} - \mathcal{A}_\mathcal{G}$, where $\mathcal{D}_\mathcal{G} = \text{diag}\{\deg_{in}(v_1), \deg_{in}(v_2), ..., \deg_{in}(v_N)\}$.

For the MAS with N agents, if an agent has one neighbour or more neighbours, we call the agent as a follower. And if an agent has no neighbour, we call it as a leader [13, 36]. Suppose that there are M leaders and $N - M$ followers, where $M < N$. Denote by $\mathcal{R} = \{1, 2, ..., M\}$ and $\mathcal{F} = \{M+1, M+2, ..., N\}$ the leader index set and the follower index set, respectively. Then, $\mathcal{L}_\mathcal{G}$ can be written as

$$L_\mathcal{G} = \begin{bmatrix} 0_{M\times M} & 0_{M\times(N-M)} \\ L_{\mathcal{F}R} & L_\mathcal{F} \end{bmatrix}, \tag{1}$$

where $L_{\mathcal{F}\mathcal{R}} \in R^{(N-M)\times M}$ and $L_\mathcal{F} \in R^{(N-M)\times(N-M)}$. Let $\tilde{\mathcal{G}}$ represent the subgraph of followers.

Assumption 1. For any given follower, it either includes no leader in its neighbour set or includes all the leaders in its neighbour set. There exists at least a follower whose neighbour set contains all leaders has a path to the follower whose neighbour set contains no leader.

Assumption 2. The subgraph $\tilde{\mathcal{G}}$ is undirected.

Remark 1. Assumption 1 is a classical assumption in the TVF tracking problems of MASs with multiple leaders and has been discussed in [23, 24]. In fact, if there are followers whose neighbour set contains some leaders instead of all leaders, then the followers' states will converge to different convex combinations. Hence, Assumption 1 ensures that followers reach an agreement on the TVF reference and maintain an offset relative to the TVF reference. Moreover, we also assume that the subgraph $\tilde{\mathcal{G}}$ is undirected to deal with the multiplicative measurement noise and get a more specific relationship between the MAS parameter and control gain.

Lemma 1([24])**.** Under Assumption 1, all the eigenvalues of $L_\mathcal{F}$ have positive real parts, and each element of $-L_\mathcal{F}^{-1}L_{\mathcal{F}\mathcal{R}}$ is identical and equals $1/M$.

The eigenvalues of $L_\mathcal{F}$ are denoted by $\lambda_1, \lambda_2, ..., \lambda_{N-M}$. Note that Assumption 1 holds. We let $0 < \text{Re}(\lambda_1) \leqslant \text{Re}(\lambda_2) \leqslant ... \leqslant \text{Re}(\lambda_{N-M})$. Moreover, if the subgraph $\tilde{\mathcal{G}}$ of followers is undirected, it is clear that the $L_\mathcal{F}$ is a symmetric matrix. Hence, all the eigenvalues of $L_\mathcal{F}$ are positive real numbers.

2.2 Problem description

We consider that the topology $\mathcal{G}$ of MASs satisfies Assumptions 1 and 2. The high-order dynamics of agent i is shown as

$$\dot{x}_i(t) = \frac{\mathrm{d}x_i(t)}{\mathrm{d}t} = Ax_i(t) + Bu_i(t), i = 1, 2, ..., N, \tag{2}$$

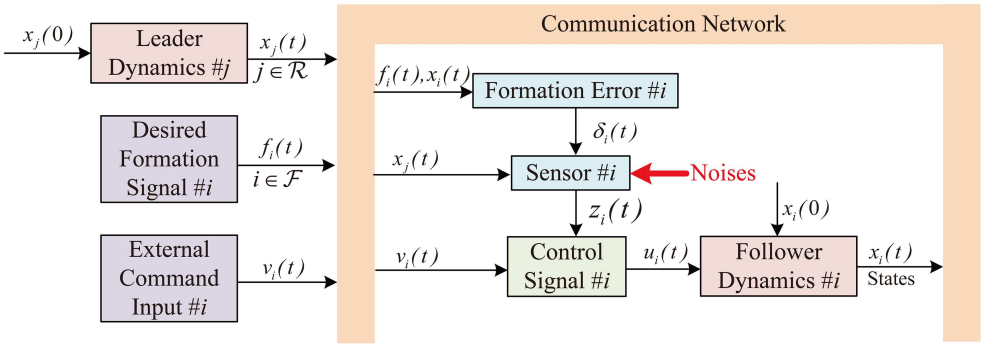

Figure 1 (Color online) The overall control structure.

where $A \in R^{n_x \times n_x}$, $B \in R^{n_x \times n_u}$ with $\text{rank}(B) = n_u$, $x_i(t) \in R^{n_x}$ and $u_i(t) \in R^{n_u}$ denote the ith agent's state and control input, respectively. Noting that $\text{rank}(B) = n_u$, there exists a nonsingular matrix $\Upsilon = [\tilde{\Upsilon}^T, \bar{\Upsilon}^T]^T$ with $\tilde{\Upsilon} \in R^{n_u \times n_x}$ and $\bar{\Upsilon} \in R^{(n_x - n_u) \times n_x}$ such that $\tilde{\Upsilon} B = I_{n_u}$ and $\bar{\Upsilon} B = 0$.

The followers are driven to realize the target TVF while tracking the convex combination of multiple leaders' states. Denoted by $f_{\mathcal{F}}(t) = [f_{M+1}^T(t), f_{M+2}^T(t), ..., f_N^T(t)]^T \in R^{(N-M)n_x}$ the target TVF of followers, where $f_i(t) \in R^{n_x}$ is continuously differentiable.

In some realistic scenarios, stochastic multiplicative noises often appear in communication process modeling [26]. Hence, we design the following TVF tracking control law/protocol with multiplicative measurement noise and illustrate its overall control structure as shown in Figure 1.

$$\begin{aligned} &u_i(t) = 0, \ i \in \mathcal{R}, && (a) \\ &u_i(t) = v_i(t) + K z_i(t), \ i \in \mathcal{F}, && (b) \end{aligned} \tag{3}$$

where $v_i(t) \in R^{n_u}$ denotes the external command input, $K \in R^{n_u \times n_x}$ is the control gain matrix, and $z_i(t)$ denotes the relative state measurement obtained by the ith agent from its neighbours. Define $\delta_i(t) = x_i(t) - f_i(t)$ $(i \in \mathcal{F})$. Then the following $z_i(t)$ is taken into account,

$$\begin{aligned} z_i(t) = &\sum_{j=1}^{M} a_{ij}[(\delta_i(t) - x_j(t)) + \sigma(\delta_i(t) - x_j(t))\varrho(t)] \\ &+ \sum_{k=M+1}^{N} a_{ik}[(\delta_i(t) - \delta_k(t)) + \sigma(\delta_i(t) - \delta_k(t))\varrho(t)], \end{aligned} \tag{4}$$

where $\sigma \geqslant 0$ denotes the finite noise intensity, $\varrho(t)$ is the independent Gaussian white noise. In this paper, the noise meets the following assumption.

Assumption 3. The noise process $\varrho(t) \in R$ satisfies

$$\int_0^t \varrho(s)\mathrm{d}s = w(t), t \geqslant 0,$$

where $w(t)$ is the independent Brownian motion defined on $(\mathbf{\Omega}, \mathbf{F}, \mathbf{P})$.

Remark 2. The TVF tracking control law/protocol (3)–(b) contains $v_i(t)$ and $Kz_i(t)$, where $v_i(t)$ is applied to expand the condition for realizing the TVF and $Kz_i(t)$ guarantees that multiple followers converge to the target TVF. In general, $z_i(t)$ is constructed by neighbour tracking error $\sum_{j=1}^{M} a_{ij}(\delta_i(t) - x_j(t))$ and neighbour relative formation error $\sum_{k=M+1}^{N} a_{ik}(\delta_i(t) - \delta_k(t))$. However, practical systems often run in uncertain communication environments and are unavoidably exposed to environmental noises. We should take the TVF problem with multiple leaders under the presence of measurement noise into account. Therefore, the measurement $z_i(t)$ is not ideal and we design a relative state measurement model with noise as shown in (4).

Let $x_{\mathcal{R}}(t) = [x_1^T(t), x_2^T(t), ..., x_M^T(t)]^T$ and $x_{\mathcal{F}}(t) = [x_{M+1}^T(t), x_{M+2}^T(t), ..., x_N^T(t)]^T$ denote the leaders' state and the followers' state, respectively. In addition, denote the convex combination of leaders as $co_{\mathcal{R}} \triangleq co\{x_1(t), x_2(t), \cdots, x_M(t)\} \triangleq \left\{\sum_{j=1}^{M} \alpha_j x_j(t), \alpha_j \geqslant 0, \ \sum_{j=1}^{M} \alpha_j = 1\right\}$. Because of the presence of

multiplicative measurement noise in the protocol (3), we have to investigate the TVF tracking problem of MAS (2) in the probability background. Then, following the definition of TVF tracking in deterministic systems [23], we give the definition of mean square TVF tracking which can also be said as TVF tracking in the mean square sense.

Definition 1. The TVF tracking in the mean square sense of MAS (2) with multiple leaders and multiplicative noise is said to be realized by $u_i(t)$ if for any initial states,

$$\lim_{t\to\infty}\mathbb{E}\|x_i(t)-f_i(t)-co_{\mathcal{R}}\|^2=0,\ i\in\mathcal{F}. \tag{5}$$

Remark 3. Definition 1 reflects that the followers keep the TVF $f_{\mathcal{F}}(t)$ in the mean square sense and come to an agreement on the convex combination of multiple leaders. For the case of only one leader, that is $M=1$, then the leader becomes the reference signal and (5) becomes $\lim_{t\to\infty}\mathbb{E}\|x_i(t)-f_i(t)-x_j(t)\|^2=0,\ i\in\mathcal{F},\ j\in\mathcal{R}$. For $f_{\mathcal{F}}(t)=0$, (5) becomes $\lim_{t\to\infty}\mathbb{E}\|x_i(t)-co_{\mathcal{R}}\|^2=0$, and then this TVF problem in Definition 1 can also be considered as a consensus problem discussed in [37]. For the case of $\lim_{t\to\infty}\sum_{i=M+1}^{N}f_i(t)=0$, it follows from (5) that $\lim_{t\to\infty}\mathbb{E}\|\sum_{i=M+1}^{N}x_i(t)/(N-M)-co_{\mathcal{R}}\|^2=0$, which indicates that the leaders' average state is at the center of $f_{\mathcal{F}}(t)$. Therefore, we can choose appropriate $f_{\mathcal{F}}(t)$ satisfying $\lim_{t\to\infty}\sum_{i=M+1}^{N}f_i(t)=0$ to solve target pursuing or target enclosing problems with multiple leaders.

2.3 Stochastic stability of SDEs

Consider establishing the mean square asymptotic stability of the following SDE:

$$\mathrm{d}z(t)=\tilde{A}z(t)\mathrm{d}t+\varphi(t)\mathrm{d}t+\mathrm{d}\mathcal{B}(t), \tag{6}$$

where $z(t),\ \varphi(t)\in R^{(N-M)n_x},\ \tilde{A}\in R^{(N-M)n_x\times(N-M)n_x},\ \mathcal{B}(t)=\int_0^t g\left(z(s)\right)\mathrm{d}w(s),\ g:R^{(N-M)n_x}\to R^{(N-M)n_x}$, $w(t)$ is the independent Brownian motion. $\mathcal{B}(t)$ is a real-valued square-integrable continuous martingale vanishing at $t=0$. The function g satisfies the following assumption.

Assumption 4. There exists a positive constant k_g such that for any $z_1,z_2\in R^{(N-M)n_x}$,

$$\|g\left(z_1\right)-g\left(z_2\right)\|\leqslant k_g\left\|z_1-z_2\right\|. \tag{7}$$

Here, for each $P>0$, there exists a matrix $D_p\geqslant 0$ such that

$$g^T(z)Pg(z)\leqslant z^TD_pz. \tag{8}$$

Remark 4. The Lipschitz condition stated in Assumption 4 is actually a very general assumption in stochastic systems. In practical scenarios, this assumption represents that noise is modeled as multiplicative in the communication process, which means that the noise intensity is proportional to the neighbour tracking error and neighbour relative formation error. Some similar assumptions can also be found in [27, 38, 39]. This assumption is to ensure the uniqueness of the closed-loop system.

Theorem 1. Suppose that Assumption 4 holds and $\lim_{t\to\infty}\varphi(t)=0$. If there exists a matrix $P>0$ such that

$$\tilde{A}^TP+P\tilde{A}+D_p<0, \tag{9}$$

then the solution to SDE (6) is mean square asymptotically stable. That is, $\lim_{t\to\infty}\mathbb{E}\|z(t)\|^2=0$.

Proof. See Appendix A.

Remark 5. For the stochastic differential delay equation, Zong et al. [38] presented the mean square and almost sure exponential stability theorem and applied it to stochastic consensus issues for MASs with multiplicative noises. Due to the existence of the deterministic term $\varphi(t)$, the existing analysis technique in [38] is no longer applicable to our current SDE. Theorem 1 establishes the new stochastic stability of SDE (6), which is used to address the TVF tracking issues in the sequel. This is also a new supplement to the stability theory of stochastic differential systems.

3 Main results

In this section, in terms of the consensus-based method, we convert the TVF tracking problem of MAS (2) with multiple leaders and multiplicative measurement noise into a mean square asymptotic stability problem. Sufficient conditions are deduced by stabilizing the corresponding closed-loop stochastic systems.

Denote $v_{\mathcal{F}}(t) = [v_{M+1}^T(t), v_{M+2}^T(t), ..., v_N^T(t)]^T$. Substituting TVF tracking protocol (3) into MAS (2), the MAS can be written as

$$\begin{cases} \dot{x}_{\mathcal{R}}(t) = (I_M \otimes A)\, x_{\mathcal{R}}(t), \\ \mathrm{d}x_{\mathcal{F}}(t) = (I_{N-M} \otimes B) v_{\mathcal{F}}(t)\mathrm{d}t - (L_{\mathcal{F}} \otimes BK) f_{\mathcal{F}}(t)\mathrm{d}t + (L_{\mathcal{FR}} \otimes BK) x_{\mathcal{R}}(t)\mathrm{d}t \\ \qquad\qquad + (I_{N-M} \otimes A + L_{\mathcal{F}} \otimes BK)\, x_{\mathcal{F}}(t)\mathrm{d}t + \mathrm{d}M_1(t), \end{cases} \tag{10}$$

where $M_1(t) = \sigma \int_0^t [(L_{\mathcal{FR}} \otimes BK) x_{\mathcal{R}}(s) + (L_{\mathcal{F}} \otimes BK)(x_{\mathcal{F}}(s) - f_{\mathcal{F}}(s))]\mathrm{d}w(s)$. Let $\delta_{\mathcal{F}}(t) = [\delta_{M+1}^T(t), \delta_{M+2}^T(t), ..., \delta_N^T(t)]^T$. Then, $\delta_{\mathcal{F}}(t) = x_{\mathcal{F}}(t) - f_{\mathcal{F}}(t)$ and (10) is converted into

$$\mathrm{d}x_{\mathcal{R}}(t) = (I_M \otimes A)\, x_{\mathcal{R}}(t)\mathrm{d}t, \tag{11}$$

$$\begin{aligned} \mathrm{d}\delta_{\mathcal{F}}(t) =& (I_{N-M} \otimes B) v_{\mathcal{F}}(t)\mathrm{d}t + (I_{N-M} \otimes A) f_{\mathcal{F}}(t)\mathrm{d}t + (L_{\mathcal{FR}} \otimes BK) x_{\mathcal{R}}(t)\mathrm{d}t \\ & + (I_{N-M} \otimes A + L_{\mathcal{F}} \otimes BK)\, \delta_{\mathcal{F}}(t)\mathrm{d}t - (I_{N-M} \otimes I_{n_x})\mathrm{d}f_{\mathcal{F}}(t) + \mathrm{d}M_2(t), \end{aligned} \tag{12}$$

where $M_2(t) = \sigma \int_0^t [(L_{\mathcal{FR}} \otimes BK) x_{\mathcal{R}}(s) + (L_{\mathcal{F}} \otimes BK)\delta_{\mathcal{F}}(s)]\ \mathrm{d}w(s)$.

Under Assumption 1, let $T_{\mathcal{F}} = [\psi_1, \psi_2, ..., \psi_{N-M}] \in R^{(N-M)\times(N-M)}$ be a nonsingular matrix such that

$$T_{\mathcal{F}}^{-1} L_{\mathcal{F}} T_{\mathcal{F}} = \Lambda = \mathrm{diag}\{\lambda_1, \lambda_2, ..., \lambda_{N-M}\}, \tag{13}$$

where $\psi_i \in R^{N-M}$ is the eigenvector corresponding to the eigenvalue λ_i, $i = 1, 2, ..., N-M$. Moreover, $T_{\mathcal{F}}^{-1} = T_{\mathcal{F}}^T$ under Assumption 2.

For $i \in \mathcal{F}$, let

$$\varepsilon_i(t) = \sum_{j=1}^{M} a_{ij}(\delta_i(t) - x_j(t)) + \sum_{k=M+1}^{N} a_{ik}(\delta_i(t) - \delta_k(t)) \tag{14}$$

and $\varepsilon_{\mathcal{F}}(t) = [\varepsilon_{M+1}^T(t), \varepsilon_{M+2}^T(t), ..., \varepsilon_N^T(t)]^T$. Then, one has

$$\varepsilon_{\mathcal{F}}(t) = (L_{\mathcal{FR}} \otimes I_{n_x})\, x_{\mathcal{R}}(t) + (L_{\mathcal{F}} \otimes I_{n_x})\, \delta_{\mathcal{F}}(t). \tag{15}$$

From (15), one gets

$$\delta_{\mathcal{F}}(t) = \left(L_{\mathcal{F}}^{-1} \otimes I_{n_x}\right) \varepsilon_{\mathcal{F}}(t) - \left(L_{\mathcal{F}}^{-1} L_{\mathcal{FR}} \otimes I_{n_x}\right) x_{\mathcal{R}}(t). \tag{16}$$

Substituting (11), (12), and (16) into the derivative of (15) has

$$\begin{aligned} \mathrm{d}\varepsilon_{\mathcal{F}}(t) =& (L_{\mathcal{F}} \otimes B)\, v_{\mathcal{F}}(t)\mathrm{d}t - (L_{\mathcal{F}} \otimes I_{n_x})\, \mathrm{d}f_{\mathcal{F}}(t) + (L_{\mathcal{F}} \otimes A)\, f_{\mathcal{F}}(t)\mathrm{d}t \\ & + (I_{N-M} \otimes A + L_{\mathcal{F}} \otimes BK)\, \varepsilon_{\mathcal{F}}(t)\mathrm{d}t + \mathrm{d}M_3(t), \end{aligned} \tag{17}$$

where $M_3(t) = \sigma \int_0^t (L_{\mathcal{F}} \otimes BK)\varepsilon_{\mathcal{F}}(s)\mathrm{d}w(s)$.

Letting $\zeta_{\mathcal{F}}(t) = (T_{\mathcal{F}}^{-1} \otimes I_{n_x})\varepsilon_{\mathcal{F}}(t) = [\zeta_{M+1}^T(t), \zeta_{M+2}^T(t), ..., \zeta_N^T(t)]^T$, then (17) is written as

$$\begin{aligned} \mathrm{d}\zeta_{\mathcal{F}}(t) =& (T_{\mathcal{F}}^{-1} L_{\mathcal{F}} \otimes B) v_{\mathcal{F}}(t)\mathrm{d}t - (T_{\mathcal{F}}^{-1} L_{\mathcal{F}} \otimes I_{n_x})\mathrm{d}f_{\mathcal{F}}(t) + (T_{\mathcal{F}}^{-1} L_{\mathcal{F}} \otimes A) f_{\mathcal{F}}(t)\mathrm{d}t \\ & + (I_{N-M} \otimes A + \Lambda \otimes BK)\, \zeta_{\mathcal{F}}(t)\mathrm{d}t + \mathrm{d}M_4(t), \end{aligned} \tag{18}$$

where $M_4(t) = \sigma \int_0^t (\Lambda \otimes BK)\zeta_{\mathcal{F}}(s)\mathrm{d}w(s)$.

Let $\tilde{A} = I_{N-M} \otimes A + \Lambda \otimes BK$ and $\varphi(t) = (T_{\mathcal{F}}^{-1} L_{\mathcal{F}} \otimes B) v_{\mathcal{F}}(t) - (T_{\mathcal{F}}^{-1} L_{\mathcal{F}} \otimes I_{n_x}) \dot{f}_{\mathcal{F}}(t) + (T_{\mathcal{F}}^{-1} L_{\mathcal{F}} \otimes A) f_{\mathcal{F}}(t)$. Hence, in noisy environments, the TVF tracking problem of MAS (2) is converted into a stochastic stability issue of (18) in terms of the above analysis. Next, Theorem 1 will be used to address stability issues, which also addresses TVF tracking issues. We will give sufficient conditions related to the control gains by stabilizing the system (18).

For the case of unstable A, namely, $\max(\mathrm{Re}(\lambda(A))) \geqslant 0$, define $\{\lambda_i^\vartheta(A)\}_i$ as the unstable eigenvalues of A and let $\lambda_0^\vartheta = \sum_i \mathrm{Re}(\lambda_i^\vartheta(A))$. In this case, the following theorem is given based on the generalized algebraic Riccati equation (GARE) [38]

$$A^TP + PA - 2\alpha PB\left(I_{n_u} + B^TPB\right)^{-1}B^TP = -I_{n_x}, \tag{19}$$

where $\alpha > \lambda_0^\vartheta$.

Theorem 2. Suppose that Assumptions 1, 2 and 3 hold, $\max(\mathrm{Re}(\lambda(A))) \geqslant 0$. Then, the proposed protocol (3) with $K = k(I_{n_u} + B^TPB)^{-1}B^TP$, $k \in (k_1, k_2)$, ensures that MAS (2) realizes the TVF tracking in the mean square sense if

(i) $\lim_{t\to\infty}\left(\bar{\Upsilon}Af_i(t) - \bar{\Upsilon}\dot{f}_i(t)\right) = 0$, $i \in \mathcal{F}$;

(ii) (A, B) is controllable;

(iii) $1 > 2\sigma^2\lambda_0^\vartheta$,

where $k_1 = \frac{-1-\sqrt{1-2\sigma^2\alpha}}{\sigma^2\lambda_{N-M}}$, $k_2 = \frac{-1+\sqrt{1-2\sigma^2\alpha}}{\sigma^2\lambda_{N-M}}$, $P > 0$ is the solution to (19) with $\alpha \in (\lambda_0^\vartheta, \frac{1}{2\sigma^2})$.

Proof. We will prove the mean square asymptotic stability of (18) under conditions (i)–(iii) by using Theorem 1. First, we give that condition (i) can deduce $\lim_{t\to\infty}\varphi(t) = 0$. If condition (i) holds for $\forall i \in \mathcal{F}$, we obtain from $\bar{\Upsilon}B = 0$ that

$$\lim_{t\to\infty}\left(\bar{\Upsilon}Bv_i(t) - \bar{\Upsilon}\dot{f}_i(t) + \bar{\Upsilon}Af_i(t)\right) = 0. \tag{20}$$

Similarly to [40], we choose a suitable $v_i(t)$ satisfying

$$\lim_{t\to\infty}\left(v_i(t) - \tilde{\Upsilon}\dot{f}_i(t) + \tilde{\Upsilon}Af_i(t)\right) = 0. \tag{21}$$

Then we can derive (22) from (20) and (21):

$$\lim_{t\to\infty}\left(\Upsilon Bv_i(t) - \Upsilon\dot{f}_i(t) + \Upsilon Af_i(t)\right) = 0. \tag{22}$$

We pre-multiply Υ^{-1} on both sides of (22) to obtain

$$\lim_{t\to\infty}\left(Bv_i(t) - \dot{f}_i(t) + Af_i(t)\right) = 0, \tag{23}$$

which means that

$$\lim_{t\to\infty}\left((I_{N-M}\otimes B)v_{\mathcal{F}}(t) - (I_{N-M}\otimes I_{n_x})\dot{f}_{\mathcal{F}}(t) + (I_{N-M}\otimes A)f_{\mathcal{F}}(t)\right) = 0. \tag{24}$$

We pre-multiply $T_{\mathcal{F}}^{-1}L_{\mathcal{F}}\otimes I_{n_x}$ on both sides of (24) to yield $\lim_{t\to\infty}\varphi(t) = 0$.

Let $\bar{P} = I_{N-M}\otimes P$ and $V(\zeta_{\mathcal{F}}(t)) = \zeta_{\mathcal{F}}^T(t)\bar{P}\zeta_{\mathcal{F}}(t)$. Note that $\mathrm{d}\langle M_4, \bar{P}M_4\rangle(t) = \zeta_{\mathcal{F}}^T(t)D_p\zeta_{\mathcal{F}}(t)\mathrm{d}t$, where $D_p = \sigma^2\Lambda^2\otimes K^TB^TPBK$. Then, we prove that conditions (i)–(iii) under $K = k(I_{n_u} + B^TPB)^{-1}B^TP$ imply $\tilde{A}^T\bar{P} + \bar{P}\tilde{A} + D_p < 0$. Note that this can be ensured by

$$(A + \lambda_iBK)^TP + P(A + \lambda_iBK) + \lambda_i^2\sigma^2K^TB^TPBK < 0, i = 1, 2, ..., N-M. \tag{25}$$

Substituting $K = k(I_{n_u} + B^TPB)^{-1}B^TP$ into (25) produces

$$\begin{aligned}\Gamma_i := A^TP + PA &+ 2\lambda_ikPB\left(I_{n_u} + B^TPB\right)^{-1}B^TP \\ &+ \lambda_i^2\sigma^2K^TB^TPBK, i = 1, 2, ..., N-M.\end{aligned}$$

Note that

$$\begin{aligned}K^TB^TPBK &= k^2PB\left(I_{n_u} + B^TPB\right)^{-1}B^TPB\left(I_{n_u} + B^TPB\right)^{-1}B^TP \\ &= k^2PB\left(I_{n_u} + B^TPB\right)^{-1}B^TP \\ &\quad - k^2PB\left(I_{n_u} + B^TPB\right)^{-1}\left(I_{n_u} + B^TPB\right)^{-1}B^TP \\ &< k^2PB\left(I_{n_u} + B^TPB\right)^{-1}B^TP.\end{aligned}$$

Then, one has

$$\Gamma_i < A^TP + PA + \kappa_i PB\left(I_{n_u} + B^TPB\right)^{-1}B^TP < 0, \tag{26}$$

where $\kappa_i = 2\lambda_i k + \sigma^2\lambda_i^2 k^2$. Due to $P > 0$ is the solution to (19), we can obtain

$$\Gamma_i < (2\alpha + \kappa_i)\, PB\left(I_{n_u} + B^TPB\right)^{-1}B^TP - I_{n_x}. \tag{27}$$

For $k \in (k_1, k_2)$, one gets $2\alpha + \kappa_i < 0$, where the condition (iii) implies that k_1 and k_2 are well defined. Then from (27), we have $\Gamma_i < 0$. Hence, by Theorem 1, (18) is mean square asymptotically stable and $\lim_{t\to\infty}\mathbb{E}\|\zeta_{\mathcal{F}}(t)\|^2 = 0$.

Finally, we further verify that the TVF tracking is realized. Note that $T_{\mathcal{F}}$ is nonsingular. We get $\lim_{t\to\infty}\mathbb{E}\|\varepsilon_{\mathcal{F}}(t)\|^2 = 0$. Then, one gets from (15) that

$$\lim_{t\to\infty}\mathbb{E}\|\left(L_{\mathcal{FR}}\otimes I_{n_x}\right)x_{\mathcal{R}}(t) + \left(L_{\mathcal{F}}\otimes I_{n_x}\right)\delta_{\mathcal{F}}(t)\|^2 = 0. \tag{28}$$

Since Assumption 1 holds, $L_{\mathcal{F}}$ is invertible. So (28) yields

$$\lim_{t\to\infty}\mathbb{E}\|x_{\mathcal{F}}(t) - f_{\mathcal{F}}(t) - (-L_{\mathcal{F}}^{-1}L_{\mathcal{FR}}\otimes I_{n_x})x_{\mathcal{R}}(t)\|^2 = 0. \tag{29}$$

Then, it holds from Lemma 1 and (29) that

$$\lim_{t\to\infty}\mathbb{E}\|x_i(t) - f_i(t) - \frac{1}{M}\sum_{j=1}^{M}x_j(t)\|^2 = 0,\ i\in\mathcal{F}, \tag{30}$$

which means that MAS (2) realizes the mean square TVF tracking.

For the case of stable A, namely, $\max(\mathrm{Re}(\lambda(A))) < 0$, the theorem is given for MAS (2) to realize the TVF tracking control as follows.

Theorem 3. Suppose that Assumptions 1, 2 and 3 hold, $\max(\mathrm{Re}(\lambda(A))) < 0$. Then, the proposed protocol (3) with $K = kB^TP$ ensures that MAS (2) realizes the TVF tracking in the mean square sense if

$$\lim_{t\to\infty}\left(\bar{\Upsilon}Af_i(t) - \bar{\Upsilon}\dot{f}_i(t)\right) = 0, i\in\mathcal{F},$$

where k meets $\lambda_{N-M}|k|\left\|PBB^TP\right\|(\sigma^2\lambda_{N-M}|k|\left\|BB^TP\right\| + 2) < 1$, $P = \int_0^\infty \mathrm{e}^{A^Tt}\mathrm{e}^{At}\mathrm{d}t$.

Proof. Similarly to (20)–(24), it holds from condition ① that $\lim_{t\to\infty}\varphi(t) = 0$. Note that A is stable. The positive definite matrix P satisfies $A^TP + PA = -I_{n_x}$. In fact, $P = \int_0^\infty \mathrm{e}^{A^Tt}\mathrm{e}^{At}\mathrm{d}t$. Choose the Lyapunov function $V(t) = \zeta_{\mathcal{F}}^T(t)\left(I_{N-M}\otimes P\right)\zeta_{\mathcal{F}}(t)$. The control gain is designed as $K = kB^TP$. Then, applying Itô formula to $V(t)$, we obtain

$$\begin{aligned}\mathrm{d}V(t) =& -\|\zeta_{\mathcal{F}}(t)\|^2\mathrm{d}t + 2k\zeta_{\mathcal{F}}^T(t)(\Lambda\otimes PBB^TP)\zeta_{\mathcal{F}}(t)\mathrm{d}t + 2\zeta_{\mathcal{F}}^T(t)(I_{N-M}\otimes P)\varphi(t)\mathrm{d}t\\ &+ \mathrm{d}m(t) + \mathrm{d}\langle M_4, (I_{N-M}\otimes P)M_4\rangle(t)\\ \leqslant& \left(2\lambda_{N-M}|k|p_b + \sigma^2\lambda_{N-M}^2k^2p_b\left\|BB^TP\right\| - 1 + \gamma\|P\|\right)\|\zeta_{\mathcal{F}}(t)\|^2\mathrm{d}t\\ &+ \frac{1}{\gamma}\varphi(t)^T(I_{N-M}\otimes P)\varphi(t)\mathrm{d}t + \mathrm{d}m(t),\end{aligned}$$

where $p_b = \left\|PBB^TP\right\|$, $m(t) = 2\int_0^t\zeta_{\mathcal{F}}^T(s)(I_{N-M}\otimes P)\mathrm{d}M_4(s)$. Then, for any $\gamma > 0$, one has

$$\begin{aligned}\mathrm{d}\left[\mathrm{e}^{\gamma t}V(t)\right] \leqslant& \gamma\mathrm{e}^{\gamma t}V(t)\,\mathrm{d}t + C_1\mathrm{e}^{\gamma t}\|\zeta_{\mathcal{F}}(t)\|^2\mathrm{d}t + \mathrm{e}^{\gamma t}\mathrm{d}m(t)\\ &+ \frac{\|P\|}{\gamma}\mathrm{e}^{\gamma t}\|\varphi(t)\|^2\,\mathrm{d}t,\end{aligned} \tag{31}$$

where $C_1 = 2\lambda_{N-M}|k|p_b + \sigma^2\lambda_{N-M}^2k^2p_b\left\|BB^TP\right\| - 1 + \gamma\|P\|$. Integrating on both sides of (31) and taking the expectations, we obtain

$$\begin{aligned}\mathrm{e}^{\gamma t}\mathbb{E}V(t) \leqslant& V(0) + \gamma\int_0^t\mathrm{e}^{\gamma s}\mathbb{E}V(s)\mathrm{d}s + C_1\int_0^t\mathrm{e}^{\gamma s}\mathbb{E}\|\zeta_{\mathcal{F}}(s)\|^2\mathrm{d}s\\ &+ \frac{\|P\|}{\gamma}\int_0^t\mathrm{e}^{\gamma s}\|\varphi(s)\|^2\,\mathrm{d}s.\end{aligned} \tag{32}$$

Algorithm 1 TVF tracking algorithm for MASs with multiple leaders and multiplicative noise.

Initialize A, B, $x_i(0)$, $\sigma > 0$;
for each agent $i \in \mathcal{F}$ **do**
  Select the target TVF $f_i(t) \in R^{n_x}$;
  if $\max(\mathrm{Re}(\lambda(A))) \geqslant 0$ **then**
    Select $\bar{\Upsilon}$ and $\tilde{\Upsilon}$ such that $\tilde{\Upsilon}B = I_{n_u}$ and $\bar{\Upsilon}B = 0$; then find a suitable $v_i(t)$ using (21);
    if conditions (i)–(iii) are satisfied **then**
      Choose $\alpha \in (\lambda_0^{\vartheta}, \frac{1}{2\sigma^2})$;
      Get P by solving the GARE (19);
      Compute $K = k(I_{n_u} + B^TPB)^{-1}B^TP$ with $k \in (k_1, k_2)$;
    else
      Go back to step 3;
    end if
  else {$\max(\mathrm{Re}(\lambda(A))) < 0$}
    Select $\bar{\Upsilon}$ and $\tilde{\Upsilon}$ such that $\tilde{\Upsilon}B = I_{n_u}$ and $\bar{\Upsilon}B = 0$; then find a suitable $v_i(t)$ using (21);
    if condition ① is satisfied **then**
      Get $P = \int_0^{\infty} \mathrm{e}^{A^Tt}\mathrm{e}^{At}\mathrm{d}t$;
      Compute $K = kB^TP$ with k satifying $\lambda_{N-M}|k|\|PBB^TP\|(\sigma^2\lambda_{N-M}|k|\|BB^TP\| + 2) < 1$;
    else
      Go back to step 3;
    end if
  end if
end for

Note that $\lambda_{\min}(P)\|\zeta_{\mathcal{F}}(t)\|^2 \leqslant V(t) \leqslant \lambda_{\max}(P)\|\zeta_{\mathcal{F}}(t)\|^2$. Then, one gets

$$\mathrm{e}^{\gamma t}\mathbb{E}V(t) \leqslant V(0) + C_2(\gamma)\int_0^t \mathrm{e}^{\gamma s}\mathbb{E}\|\zeta_{\mathcal{F}}(s)\|^2\mathrm{d}s + \frac{\|P\|}{\gamma}\int_0^t \mathrm{e}^{\gamma s}\|\varphi(s)\|^2\mathrm{d}s, \tag{33}$$

where $C_2(\gamma) = C_1 + \lambda_{\max}(P)\gamma$. Note that $C_2(0) = 2\lambda_{N-M}|k|p_b + \sigma^2\lambda_{N-M}^2k^2p_b\left\|BB^TP\right\| - 1 < 0$ and $C_2(\gamma_1) > 0$, where $\gamma_1 > \frac{-\left(2\lambda_{N-M}|k|p_b+\sigma^2\lambda_{N-M}^2k^2p_b\left\|BB^TP\right\|-1\right)}{\lambda_{\max}(P)+\|P\|}$. Therefore, there exists a $\tilde{\gamma}$ such that $C_2(\tilde{\gamma}) = 0$. Then, it holds from (33) that

$$\mathrm{e}^{\tilde{\gamma}t}\mathbb{E}V(t) \leqslant V(0) + \frac{\|P\|}{\gamma}\int_0^t \mathrm{e}^{\tilde{\gamma}s}\|\varphi(s)\|^2\mathrm{d}s. \tag{34}$$

Then, we can obtain $\lambda_{\min}(P)\mathrm{e}^{\tilde{\gamma}t}\mathbb{E}\|\zeta_{\mathcal{F}}(t)\|^2 \leqslant V(0) + \frac{\|P\|}{\gamma}\int_0^t \mathrm{e}^{\tilde{\gamma}s}\|\varphi(s)\|^2\mathrm{d}s$. That is

$$\mathbb{E}\|\zeta_{\mathcal{F}}(t)\|^2 \leqslant \frac{\mathrm{e}^{-\tilde{\gamma}t}V(0)}{\lambda_{\min}(P)} + \frac{\|P\|}{\lambda_{\min}(P)\gamma}\int_0^t \mathrm{e}^{\tilde{\gamma}(s-t)}\|\varphi(s)\|^2\mathrm{d}s.$$

From $\lim_{t\to\infty}\varphi(t) = 0$, we have $\lim_{t\to\infty}\int_0^t \mathrm{e}^{\tilde{\gamma}(s-t)}\|\varphi(s)\|^2 d\mathrm{d}s = 0$. Hence, one has $\lim_{t\to\infty}\mathbb{E}\|\zeta_{\mathcal{F}}(t)\|^2 = 0$ and $\lim_{t\to\infty}\mathbb{E}\|\varepsilon_{\mathcal{F}}(t)\|^2 = 0$. Similarly to (28)–(30), we obtain that MAS (2) with multiple leaders and multiplicative noise realizes the mean square TVF tracking.

Following Theorems 2 and 3, calculating steps for followers to realize the mean square TVF tracking are given in Algorithm 1.

Remark 6. $\lim_{t\to\infty}\left(\bar{\Upsilon}Af_i(t) - \bar{\Upsilon}\dot{f}_i(t)\right) = 0$ in Theorems 2 and 3 are formation tracking feasibility conditions, which reveals that not all the given formation shapes can be realized by the followers. The feasible TVF vectors need to satisfy the constraints on the dynamics of each agent. Therefore, the shape, size, and orientation of the TVF can be varied by choosing different $f_F(t)$ without redesigning the TVF tracking control law/protocol.

Remark 7. For unstable A, Theorem 2 gives sufficient conditions for the realization of the TVF tracking and proves that the control gain $K = k(I_{n_u} + B^TPB)B^TP$ can be applied to stabilize the closed-loop stochastic system (18), where matrix P is a unique solution of GARE (19) and can be solved in MATLAB with the help of the method mentioned in [38]. For stable A, Theorem 3 also gives corresponding sufficient conditions and proves that the control gain $K = kB^TP$ can stabilize (18), where P is determined only by A. Through the results, it can be observed that for stable A, the mean square TVF tracking can be realized at any noise intensity by designing the control gain to eliminate the effect of multiplicative measurement noise.

Remark 8. For the case of target TVF $f_{\mathcal{F}}(t) = 0$, this TVF tracking problem can be considered as a multiple leaders' containment control problem for MAS under multiplicative measurement noise. That is,

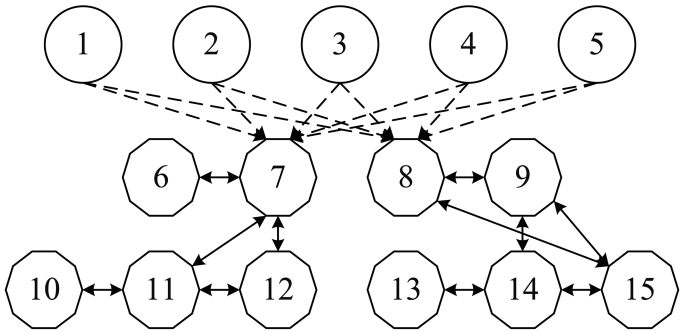

Figure 2 Communication topology $\mathcal{G}_1$.

Theorems 2 and 3 can be applied to settle multiple leaders' containment matter of MASs with stochastic noise.

4 Simulations

In this section, the designed TVF tracking strategy is used for settling the MAS TVF matters and two simulation examples are given by using the Euler-Maruyama method [39].

Example 1. Consider the third-order MAS with 5 leaders and 10 followers and its communication topology $\mathcal{G}_1$ as shown in Figure 2. The dynamics of each agent is described by (2) with $x_i(t) = [x_{i1}(t), x_{i2}(t), x_{i3}(t)]^T$ $(i = 1, 2, ..., 15)$ and

$$A = \begin{bmatrix} 0 & 1 & 1 \\ 1 & 2 & 1 \\ -2 & -6 & -3 \end{bmatrix}, B = \begin{bmatrix} -1 & 0 \\ 0 & 1 \\ 1 & -1 \end{bmatrix}.$$

Set the simulation time to 45 s and the period of sample to 0.1 s. Let the initial states of agents be $x_i(0) = \left[\sin\left(\frac{(-2+2i)}{5}\pi\right), \cos\left(\frac{(-2+2i)}{5}\pi\right), 2\cos\left(\frac{(-2+2i)}{5}\pi\right)\right]^T$ $(i = 1, \ldots, 5)$ and $x_i(0) = \left[3\sin\left(\frac{(-1+i)}{5}\pi\right), -3\cos\left(\frac{(-1+i)}{5}\pi\right), 6\cos\left(\frac{(-1+i)}{5}\pi\right)\right]^T$ $(i = 6, \ldots, 15)$. In order to demonstrate the effect of noise intensity in this example, we present two cases: $\sigma = 0.1$ and $\sigma = 0.3$, respectively.

The followers are required to form the following target TVF:

$$f_i(t) = \begin{bmatrix} 10\sin\left(t + \frac{(-1+i)}{5}\pi\right) \\ -10\cos\left(t + \frac{(-1+i)}{5}\pi\right) \\ 20\cos\left(t + \frac{(-1+i)}{5}\pi\right) \end{bmatrix}, \ i = 6, \ldots, 15.$$

From $f_i(t)$, it is observed that when the target TVF is realized, the 10 followers will maintain the shape of a regular decagon while tracking the convex combination formed by 5 leaders.

Noting $\max(\mathrm{Re}(\lambda(A))) = 0$, we will select the parameters and design the control gain according to Theorem 2. Choosing $\tilde{\Upsilon} = [0, 1, 1; 1, 2, 1]$ and $\bar{\Upsilon} = [1, 1, 1]$, which ensures that condition (i) in Theorem 2 holds; then $v_i(t)$ is calculated from (21) as $v_i(t) = 0$. For the case of $\sigma = 0.1$, we choose $\alpha = 1$ satisfying $(\lambda_0^{\vartheta}, \frac{1}{2\sigma^2}) = (0, 50)$, P is solved by the GARE (19) as $P = [2.0746, 2.7619, 1.3380; 2.7619, 7.6767, 2.2056; 1.3380, 2.2056, 1.2981]$. We choose $k = -2.5$ satisfying $(k_1, k_2) = (-23.6086, -0.1192)$. Then the control gain in Theorem 2 is calculated as $K = [0.9164, 0.0734, -0.0673; \ -0.5548, -2.4516, -0.4140]$. For the case of $\sigma = 0.3$, we also choose $\alpha = 1$ and $k = -2.5$. It is clear that $\alpha \in (\lambda_0^{\vartheta}, \frac{1}{2\sigma^2}) = (0, 5.5556)$ and $k \in (k_1, k_2) = (-2.5119, -0.1245)$; the solutions of P and K are now the same as those in the case of $\sigma = 0.1$.

By selecting a sample path, we obtain Figures 3–5. Figure 3 displays the trajectories of all the agents in $\sigma = 0.1$ and $\sigma = 0.3$. It shows that 10 followers realize the circular TVF. Figure 4 shows trajectory

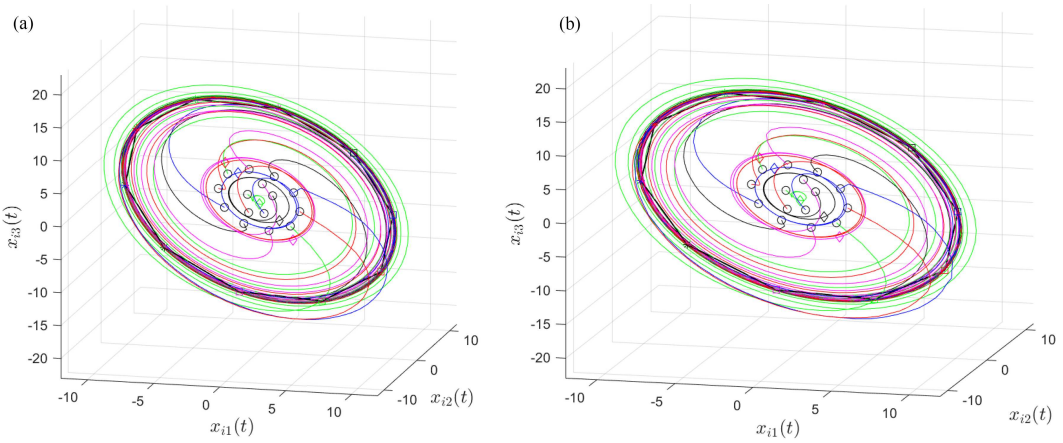

Figure 3 (Color online) Trajectories of all the agents in Example 1, where circles denote the initial states of agents, asterisks and squares denote the final states of followers, and diamonds denote the final states of leaders. (a) $\sigma = 0.1$; (b) $\sigma = 0.3$.

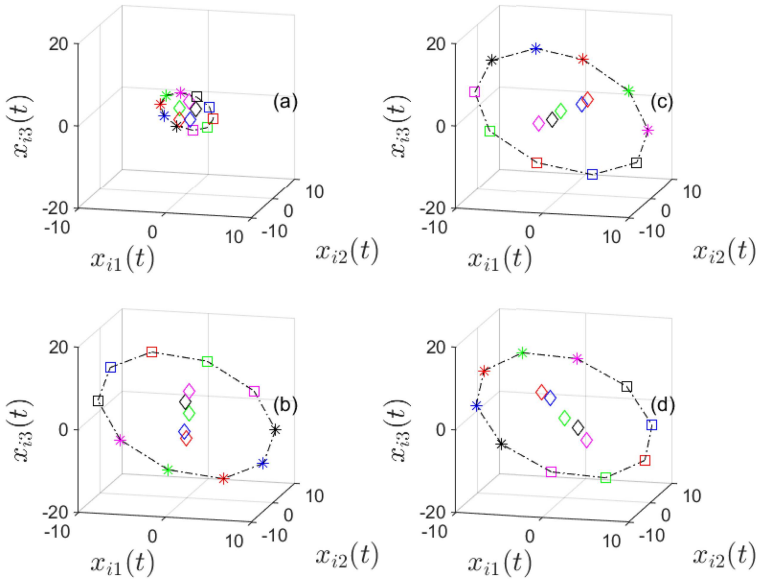

Figure 4 (Color online) Trajectory snapshots of all the agents for $\sigma = 0.3$ in Example 1: (a) t=0 s; (b) t=15 s; (c) t=30 s; (d) t=45 s. Asterisks and squares denote the states of followers and diamonds denote the states of leaders.

snapshots of 5 leaders and 10 followers at four different instants. The results show that 10 followers can maintain a regular decagonal formation and keep rotating around the convex combination of 5 leaders. Figure 5 displays the TVF tracking error curves of 10 followers, it is clear that all the curves converge to zero at about 7 s and followers realize the TVF tracking. Moreover, it can be seen that a large noise intensity will make the follower's state produce more fluctuations. For the mean square TVF tracking, we generate 1000 sample paths. Taking the mean square average, the mean square TVF tracking error curve $\mathbb{E}\|\varepsilon_{\mathcal{F}}(t)\|^2$ for $\sigma = 0.3$ is obtained in Figure 6, which reflects that followers eventually realize the mean square TVF tracking.

Example 2. Consider a second-order unmanned aerial vehicle (UAV) swarm system with 3 leaders and 5 followers in the XYZ plane. The communication topology is shown in Figure 7. The dynamics of each UAV is described by (2) with $x_i(t) = [x_{iX}(t), v_{iX}(t), x_{iY}(t), v_{iY}(t), x_{iZ}(t), v_{iZ}(t)]^T$ $(i = 1, \ldots, 8)$ and

$$A = I_3 \otimes \begin{bmatrix} 0 & 1 \\ 0 & 0 \end{bmatrix}, B = I_3 \otimes \begin{bmatrix} 0 \\ 1 \end{bmatrix}.$$

Assume the noise intensity is $\sigma = 0.3$.

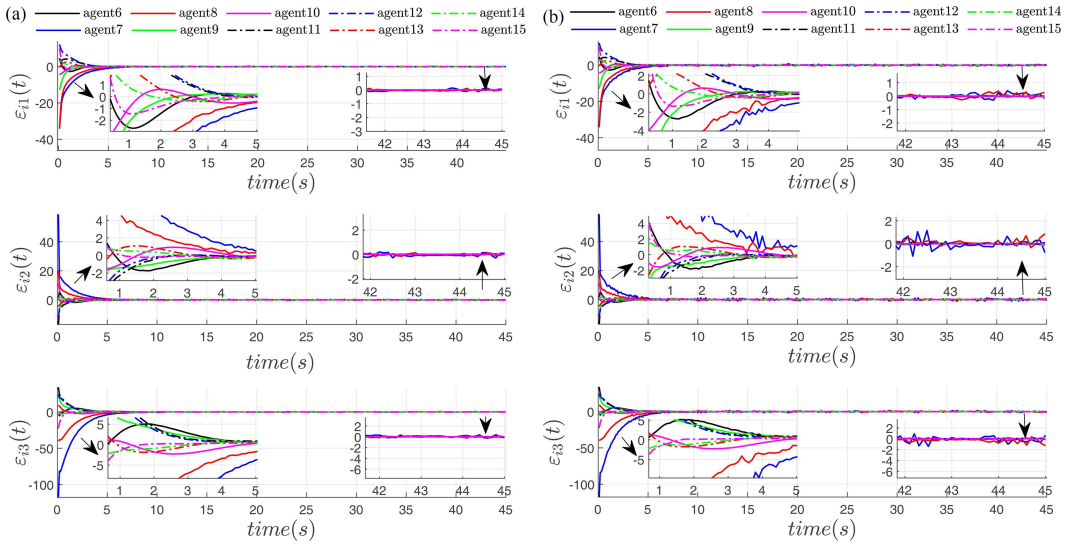

Figure 5 (Color online) TVF tracking error curves of followers in Example 1. (a) $\sigma = 0.1$; (b) $\sigma = 0.3$.

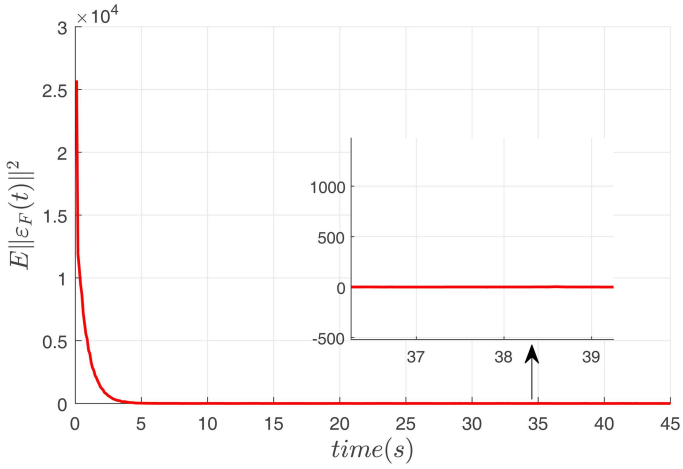

Figure 6 (Color online) Mean square tracking error $\mathbb{E}\|\varepsilon_{\mathcal{F}}(t)\|^2$ for $\sigma = 0.3$ in Example 1.

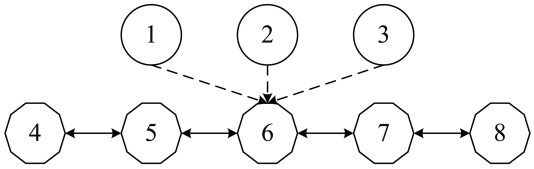

Figure 7 Communication topology $\mathcal{G}_2$.

Let the target TVF be $f_i(t) = [f_{iX}(t), f_{v_{iX}}(t), f_{iY}(t), f_{v_{iY}}(t), f_{iZ}(t), f_{v_{iZ}}(t)]^T$, which is specified by

$$f_i(t) = \begin{bmatrix} 10\sin\left(t + \frac{(-2+2i)}{5}\pi\right) \\ 10\cos\left(t + \frac{(-2+2i)}{5}\pi\right) \\ -10\cos\left(t + \frac{(-2+2i)}{5}\pi\right) \\ 10\sin\left(t + \frac{(-2+2i)}{5}\pi\right) \\ 20\cos\left(t + \frac{(-2+2i)}{5}\pi\right) \\ -20\sin\left(t + \frac{(-2+2i)}{5}\pi\right) \end{bmatrix}, \ i = 4, \ldots, 8.$$

Noting $\max(\mathrm{Re}(\lambda(A))) = 0$, we still select the parameters and design the control gain according to The-

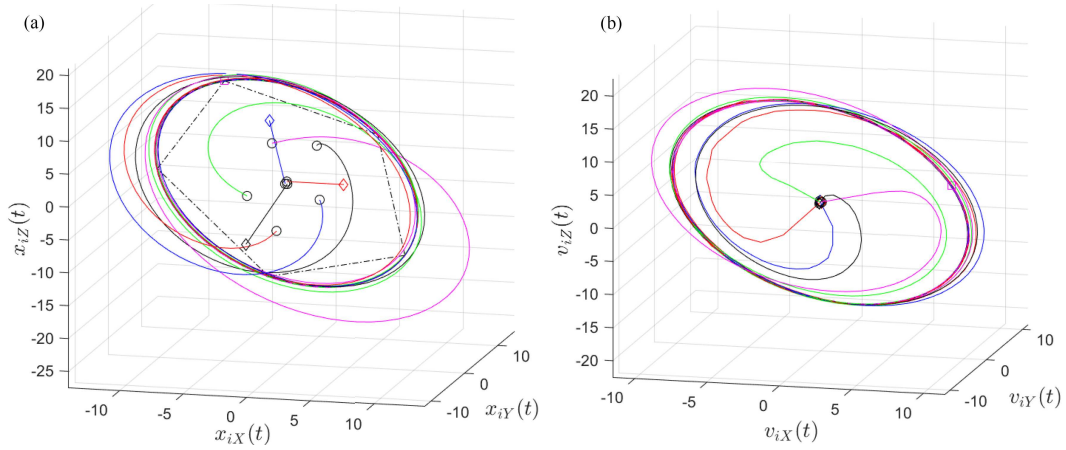

Figure 8 (Color online) Trajectories of all the UAVs with multiplicative noise in Example 2, where circles denote the initial states of UAVs, asterisks and squares denote the final states of followers, and diamonds denote the final states of leaders. (a) Position trajectories; (b) velocity trajectories.

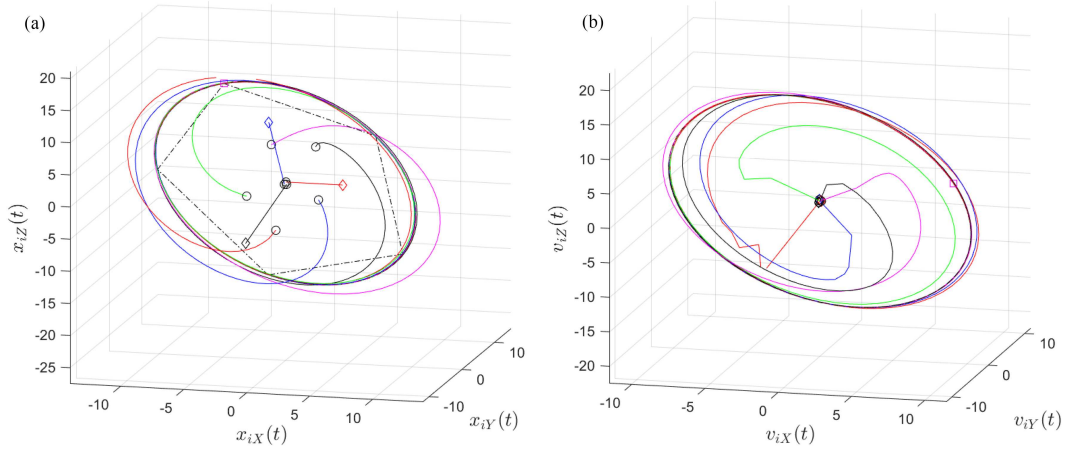

Figure 9 (Color online) Trajectories of all the UAVs without multiplicative noise in Example 2, where circles denote the initial states of UAVs, asterisks and squares denote the final states of followers, and diamonds denote the final states of leaders. (a) Position trajectories; (b) velocity trajectories.

orem 2. Choosing $\tilde{\Upsilon} = I_3 \otimes [0, 1]$ and $\bar{\Upsilon} = I_3 \otimes [1, 0]$, $v_i(t)$ is calculated as $v_i(t) = \left[-10\sin\left(t + \frac{(-2+2i)}{5}\pi\right), 10\cos\left(t + \frac{(-2+2i)}{5}\pi\right), -20\cos\left(t + \frac{(-2+2i)}{5}\pi\right)\right]^T$. Choose $\alpha = 1 \in (\lambda_0^{\vartheta}, \frac{1}{2\sigma^2}) = (0, 50)$ and $k = -3 \in (k_1, k_2) = (-3.7858, -0.1877)$. Then we calculate that $P = [1.9144, 1.3324; 1.3324, 2.5508]$ and $K = [-1.1257, -2.1551]$.

In addition, to compare with the TVF tracking in deterministic systems, we also give the simulation results for UAVs without multiplicative noise. In this case, the control protocol is designed as $K = -k[\mathrm{Re}(\lambda_1)]^{-1}B^TP$ using the method in [23], where $k > 0.5$ and P is the positive solution to $A^TP + PA - PBB^TP + I_{n_x} = 0$. Then, we obtain $K = [-2.2136, -3.8340]$.

By selecting one sample path, we obtain Figures 8–12. Figures 8 and 9 display the position and velocity trajectories for all the UAVs. It shows that follower UAVs realize a circular TVF. Figure 10 shows trajectory snapshots of 8 UAVs with multiplicative noise, which indicates that 5 followers can maintain a regular pentagon shape while rotating around the convex combination of 3 leaders. Figures 11 and 12 display the TVF tracking error curves of follower UAVs, it reveals that all the position and velocity tracking error curves converge to zero. As shown in Figure 11, the position curves are smooth and differentiable, while the velocity curves are not smooth due to the control input of velocity containing a random multiplicative noise. Moreover, by comparing the velocity curves of UAVs with noise and without noise, it can be found that under our controller, the overshoot is significantly smaller and the number of

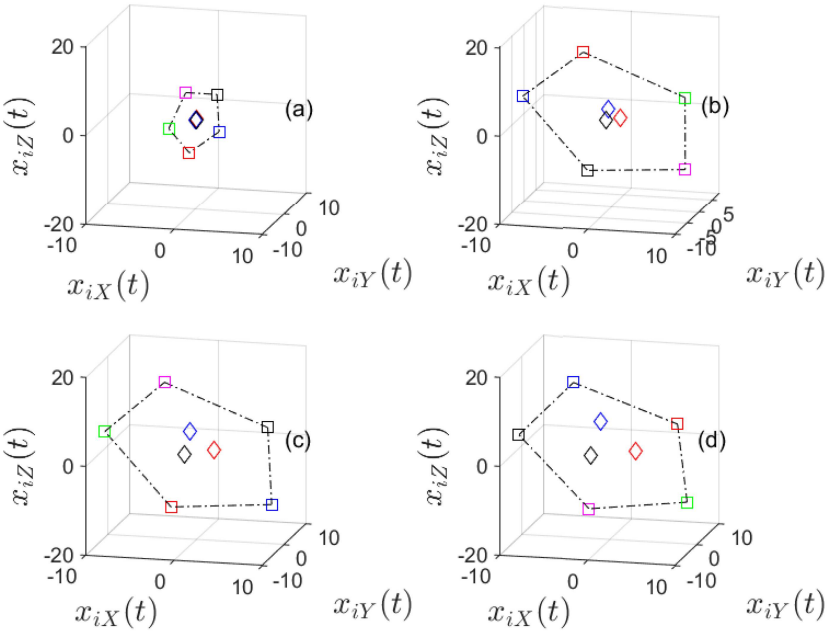

Figure 10 (Color online) Trajectory snapshots of all the UAVs with multiplicative noise in Example 2: (a) t=0 s; (b) t=15 s; (c) t=30 s; (d) t=45 s. Asterisks and squares denote the states of followers and diamonds denote the states of leaders.

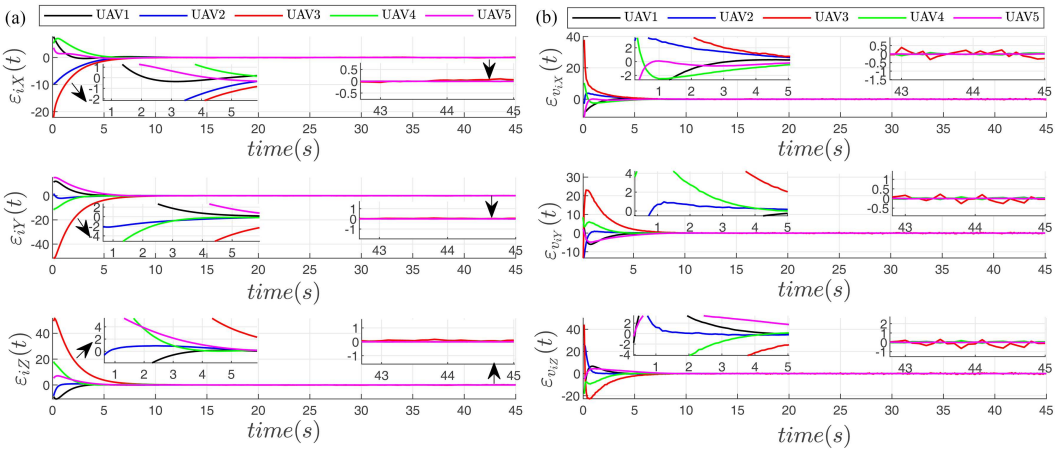

Figure 11 (Color online) TVF tracking error curves of followers with multiplicative noise in Example 2. (a) Position tracking error curves: $\varepsilon_{iX}(t)$, $\varepsilon_{iY}(t)$, and $\varepsilon_{iZ}(t)$; (b) velocity tracking error curves: $\varepsilon_{v_{iX}}(t)$, $\varepsilon_{v_{iY}}(t)$, and $\varepsilon_{v_{iZ}}(t)$.

oscillations is less before achieving the TVF tracking. For the mean square TVF tracking, we generate 1000 sample paths and obtain the mean square TVF tracking error curve $\mathbb{E}\|\varepsilon_{\mathcal{F}}(t)\|^2$ in Figure 13. It is shown that follower UAVs eventually realize the mean square TVF tracking.

5 Conclusion

The TVF tracking problem of high-order MASs under multiplicative measurement noise and multiple leaders was investigated. We developed the TVF tracking protocol with multiple leaders and multiplicative measurement noise. In terms of the consensus theory, the TVF tracking problem was converted into the stochastic stability problem. For the case of unstable A and stable A, sufficient conditions for MASs to realize the mean square TVF tracking were derived by utilizing the Lyapunov function, respectively. The obtained conclusions in the article can also be devoted to solving consensus tracking and target enclosing problems under uncertain communication environments. As a practical control problem, we

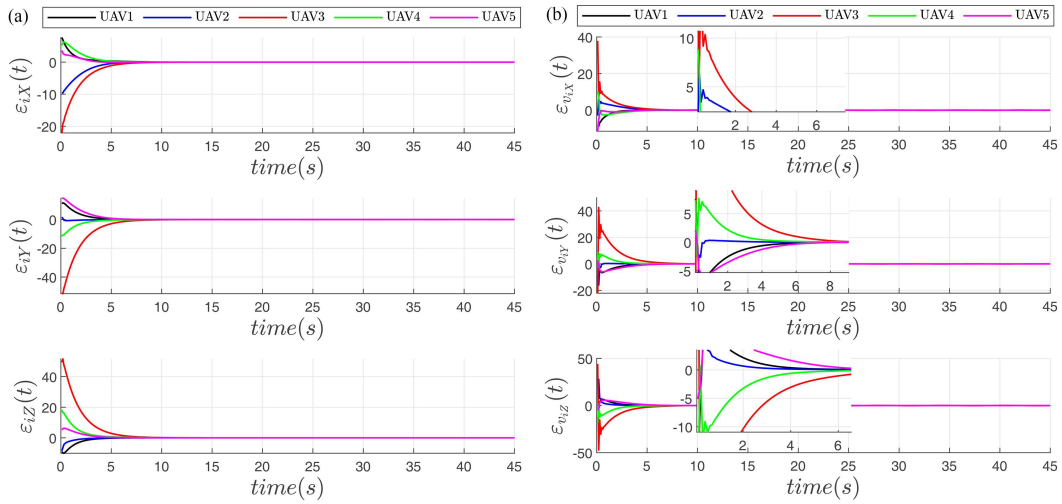

Figure 12 (Color online) TVF tracking error curves of followers without multiplicative noise in Example 2. (a) Position tracking error curves: $\varepsilon_{iX}(t)$, $\varepsilon_{iY}(t)$, and $\varepsilon_{iZ}(t)$; (b) velocity tracking error curves: $\varepsilon_{v_{iX}}(t)$, $\varepsilon_{v_{iY}}(t)$, and $\varepsilon_{v_{iZ}}(t)$.

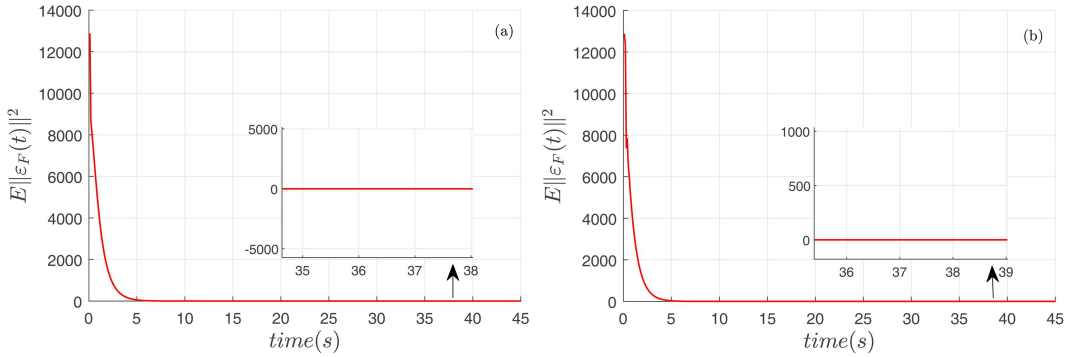

Figure 13 (Color online) Mean square tracking error $\mathbb{E}\|\varepsilon_{\mathcal{F}}(t)\|^2$ in Example 2. (a) UAVs with multiplicative noise; (b) UAVs without multiplicative noise.

will explore the stochastic TVF tracking control under more network constraints or actuator failures in the future.

Acknowledgements This work was supported by National Natural Science Foundation of China (Grant No. 62473347).

References

1 Yuan C, Licht S, He H. Formation learning control of multiple autonomous underwater vehicles with heterogeneous nonlinear uncertain dynamics. IEEE Trans Cybern, 2017, 48: 2920–2934
2 Peng Z, Wang D, Li T, et al. Output-feedback cooperative formation maneuvering of autonomous surface vehicles with connectivity preservation and collision avoidance. IEEE Trans Cybern, 2019, 50: 2527–2535
3 Wang C, Xie G, Cao M. Forming circle formations of anonymous mobile agents with order preservation. IEEE Trans Automat Contr, 2013, 58: 3248–3254
4 Nuño E, Loria A, Hernández T, et al. Distributed consensus-formation of force-controlled nonholonomic robots with time-varying delays. Automatica, 2020, 120: 109114
5 Balch T, Arkin R C. Behavior-based formation control for multirobot teams. IEEE Trans Robot Automat, 1998, 14: 926–939
6 Wang Y, Wang D. Tight formation control of multiple unmanned aerial vehicles through an adaptive control method. Sci China Inf Sci, 2017, 60: 070207
7 Wang X, Shen L, Liu Z, et al. Coordinated flight control of miniature fixed-wing UAV swarms: methods and experiments. Sci China Inf Sci, 2019, 62: 212204
8 Beard R W, Lawton J, Hadaegh F Y. A coordination architecture for spacecraft formation control. IEEE Trans Contr Syst Technol, 2001, 9: 777–790
9 Chen Q, Sun Y, Zhao M, et al. A virtual structure formation guidance strategy for multi-parafoil systems. IEEE Access, 2019, 7: 123592
10 Liang X, Liu Y H, Wang H, et al. Leader-following formation tracking control of mobile robots without direct position measurements. IEEE Trans Automat Contr, 2016, 61: 4131–4137
11 Park B S, Yoo S J. Connectivity-maintaining and collision-avoiding performance function approach for robust leader-follower formation control of multiple uncertain underactuated surface vessels. Automatica, 2021, 127: 109501
12 Trinh M H, Tran Q V, Vu D V, et al. Robust tracking control of bearing-constrained leader-follower formation. Automatica, 2021, 131: 109733

13 Liu Y, Dong X, Shi P, et al. Distributed fault-tolerant formation tracking control for multiagent systems with multiple leaders and constrained actuators. IEEE Trans Cybern, 2023, 53: 3738–3747
14 Xiao F, Wang L, Chen J, et al. Finite-time formation control for multi-agent systems. Automatica, 2009, 45: 2605–2611
15 Li X, Bai Y, Dong X, et al. Distributed time-varying formation control with uncertainties based on an event-triggered mechanism. Sci China Inf Sci, 2021, 64: 132204
16 Ren W. Consensus strategies for cooperative control of vehicle formations. IET Control Theor Appl, 2007, 1: 505–512
17 Cao Y, Ren W. Distributed formation control for fractional-order systems: dynamic interaction and absolute/relative damping. Syst Control Lett, 2010, 59: 233–240
18 Dong X, Xi J, Lu G, et al. Formation control for high-order linear time-invariant multiagent systems with time delays. IEEE Trans Control Netw Syst, 2014, 1: 232–240
19 Dong X, Shi Z, Lu G, et al. Formation-containment analysis and design for high-order linear time-invariant swarm systems. Intl J Robust NOnlinear, 2015, 25: 3439–3456
20 Han L, Dong X, Li Q, et al. Formation-containment control for second-order multi-agent systems with time-varying delays. Neurocomputing, 2016, 218: 439–447
21 Tian L, Hua Y, Dong X, et al. Distributed time-varying group formation tracking for multiagent systems with switching interaction topologies via adaptive control protocols. IEEE Trans Ind Inf, 2022, 18: 8422–8433
22 Su H, Zhang J, Chen X. A stochastic sampling mechanism for time-varying formation of multiagent systems with multiple leaders and communication delays. IEEE Trans Neural Netw Learn Syst, 2019, 30: 3699–3707
23 Dong X, Hu G. Time-varying formation tracking for linear multiagent systems with multiple leaders. IEEE Trans Automat Contr, 2017, 62: 3658–3664
24 Dong X, Tan Q, Li Q, et al. Necessary and sufficient conditions for average formation tracking of second-order multi-agent systems with multiple leaders. J Franklin Institute, 2017, 354: 611–626
25 Wang Z, Wu Y, Li T, et al. Adaptive fault-tolerant time-varying formation tracking for multiagent systems with multiple leaders. Intl J Robust Nonlinear, 2019, 29: 1807–1822
26 Ni Y H, Li X. Consensus seeking in multi-agent systems with multiplicative measurement noises. Syst Control Lett, 2013, 62: 430–437
27 Wang J, Elia N. Mitigation of complex behavior over networked systems: analysis of spatially invariant structures. Automatica, 2013, 49: 1626–1638
28 Cheng L, Hou Z G, Tan M, et al. Necessary and sufficient conditions for consensus of double-integrator multi-agent systems with measurement noises. IEEE Trans Automat Contr, 2011, 56: 1958–1963
29 Ge X, Han Q L, Yang F. Event-based set-membership leader-following consensus of networked multi-agent systems subject to limited communication resources and unknown-but-bounded noise. IEEE Trans Ind Electron, 2016, 64: 5045–5054
30 Wang B, Tian Y P. Distributed formation control: asymptotic stabilization results under local noisy information. IEEE Trans Cybern, 2019, 51: 16–27
31 Li Z, Huang T, Tang Y, et al. Formation control of multiagent systems with communication noise: a convex analysis approach. IEEE Trans Cybern, 2019, 51: 2253–2264
32 Li Z, Tang Y, Fang J, et al. Formation control of multi-agent systems with orientation noises. IEEE Trans Netw Sci Eng, 2020, 8: 305–317
33 Li B, Wen G, Peng Z, et al. Time-varying formation control of general linear multi-agent systems under Markovian switching topologies and communication noises. IEEE Trans Circuits Syst II Express Briefs, 2020, 68: 1303-1307
34 Shames I, Fidan B, Anderson B D O. Minimization of the effect of noisy measurements on localization of multi-agent autonomous formations. Automatica, 2009, 45: 1058–1065
35 Jia R, Zong X. Time-varying formation control of linear multiagent systems with time delays and multiplicative noises. Intl J Robust Nonlinear, 2021, 31: 9008–9025
36 Li W, Zhang H, Zhang J, et al. Fully distributed dynamic event-triggered formation-containment tracking for multiagent systems with multiple types of disturbances. Sci China Inf Sci, 2024, 67: 112203
37 Ren J, Zong X. Containment control of multi-agent systems with stochastic multiplicative noises. J Syst Sci Complex, 2022, 35: 909–930
38 Zong X, Li T, Yin G, et al. Stochastic consentability of linear systems with time delays and multiplicative noises. IEEE Trans Automat Contr, 2017, 63: 1059–1074
39 Mao X. Stochastic Differential Equations and Applications. Chichester, UK: Horwood Publishing Limited, 1997
40 Dong X, Hu G. Time-varying formation control for general linear multi-agent systems with switching directed topologies. Automatica, 2016, 73: 47–55

Appendix A Proof of Theorem 1

We choose the Lyapunov function $V(z_t) = z^T(t)Pz(t)$. According to the Itô formula, one gets

$$\begin{aligned} \mathrm{d}V(z_t) =& z^T(t)[\tilde{A}^T P + P\tilde{A}]z(t)\mathrm{d}t + 2z^T(t)P\varphi(t)\mathrm{d}t \\ &+ \mathrm{d}\left\langle \mathcal{B}, P\mathcal{B}\right\rangle(t) + \mathrm{d}\tilde{\mathcal{B}}(t), \end{aligned} \tag{A1}$$

where $\left\langle \mathcal{B}, P\mathcal{B}\right\rangle(t) = \int_0^t g^T(z(s))\, Pg(z(s))\,\mathrm{d}s$ and $\tilde{\mathcal{B}}(t) = 2\int_0^t z^T(s)P\mathrm{d}\mathcal{B}(s)$. Note that the elementary inequality: $2a^TOb \leqslant \epsilon a^TOa + \frac{1}{\epsilon}b^TOb$, for any positive definite matrix $O \in R^{(N-M)n_x\times(N-M)n_x}$, $\epsilon > 0$, and $a, b \in R^{(N-M)n_x}$. Then, one has

$$2z^T(t)P\varphi(t) \leqslant \gamma z^T(t)Pz(t) + \frac{1}{\gamma}\varphi^T(t)P\varphi(t) \tag{A2}$$

for any $\gamma > 0$. Then, we obtain from (8) and (A2) that

$$\begin{aligned} \mathrm{d}V(z_t) \leqslant& z^T(t)[\tilde{A}^T P + P\tilde{A} + D_p + \gamma P]z(t)\mathrm{d}t \\ &+ \frac{1}{\gamma}\varphi^T(t)P\varphi(t)\mathrm{d}t + \mathrm{d}\tilde{\mathcal{B}}(t). \end{aligned} \tag{A3}$$

Using the Itô formula to $e^{\gamma t}V(z_t)$, one has

$$\begin{aligned}\mathrm{d}\left[\mathrm{e}^{\gamma t}V(z_t)\right] &= \gamma \mathrm{e}^{\gamma t}V(z_t)\mathrm{d}t + \mathrm{e}^{\gamma t}\mathrm{d}V(z_t)\\ &\leqslant \gamma \mathrm{e}^{\gamma t}V(z_t)\mathrm{d}t + \mathrm{e}^{\gamma t}z^T(t)\Phi_1(\gamma)z(t)\mathrm{d}t\\ &\quad + \mathrm{e}^{\gamma t}\varphi^T(t)Q\varphi(t)\mathrm{d}t + \mathrm{e}^{\gamma t}\mathrm{d}\tilde{\mathcal{B}}(t),\end{aligned} \tag{A4}$$

where $\Phi_1(\gamma)=\tilde{A}^TP+P\tilde{A}+D_p+\gamma P$ and $Q=\frac{1}{\gamma}P$. Integrating on both sides of (A4) and taking the expectations, we have

$$\begin{aligned}\mathrm{e}^{\gamma t}\mathbb{E}V(z_t) \leqslant V(z_0) &+ \int_0^t \gamma \mathrm{e}^{\gamma s}\mathbb{E}V(z_s)\,\mathrm{d}s\\ &+ \mathbb{E}\int_0^t \mathrm{e}^{\gamma s}z^T(s)\Phi_1(\gamma)z(s)\mathrm{d}s\\ &+ \int_0^t \mathrm{e}^{\gamma s}\varphi^T(s)Q\varphi(s)\mathrm{d}s.\end{aligned} \tag{A5}$$

From the definition of $V(z_t)$, one yields

$$\begin{aligned}\mathrm{e}^{\gamma t}\mathbb{E}V(z_t) \leqslant V(z_0) &+ \mathbb{E}\int_0^t \mathrm{e}^{\gamma s}z^T(s)\Phi_2(\gamma)z(s)\mathrm{d}s\\ &+ \int_0^t \mathrm{e}^{\gamma s}\varphi^T(s)Q\varphi(s)\mathrm{d}s,\end{aligned} \tag{A6}$$

where $\Phi_2(\gamma)=\Phi_1(\gamma)+\gamma P$. Note that $\Phi_2(0)<0$ under (9). Hence, if (9) holds, there must be a $\bar{\gamma}>0$ such that for any $\gamma<\bar{\gamma}$, $\Phi_2(\gamma)=\tilde{A}^TP+P\tilde{A}+D_p+2\gamma P<0$. Then, we get the following from (A6):

$$\mathrm{e}^{\gamma t}\mathbb{E}V(z_t) \leqslant V(z_0) + \int_0^t \mathrm{e}^{\gamma s}\varphi^T(s)Q\varphi(s)\mathrm{d}s. \tag{A7}$$

Note that $V(t)\geqslant \lambda_{\min}(P)\|z(t)\|^2$. Together with (A7), we obtain

$$\mathbb{E}\|z(t)\|^2 \leqslant \frac{V(z_0)\mathrm{e}^{-\gamma t}}{\lambda_{\min}(P)} + \frac{\|P\|}{\lambda_{\min}(P)\gamma}\int_0^t \mathrm{e}^{\gamma(s-t)}\|\varphi(s)\|^2\mathrm{d}s.$$

We have from $\lim_{t\to\infty}\varphi(t)=0$ that $\lim_{t\to\infty}\int_0^t \mathrm{e}^{\gamma(s-t)}\ \|\varphi(s)\|^2\mathrm{e}s=0$, and then it produces $\lim_{t\to\infty}\mathbb{E}\|z(t)\|^2=0$. That is to say, the SDE (6) is mean square asymptotically stable.